The Japan Society of Mechanical Engineers

Vibrations of Nonlinear Systems with Discontinuities*
(The Case of a Preloaded Compliance System)

Yutaka YOSHITAKE**, Atsuo SUEOKA***,
Nobuchika SHOJI**** and Toshitaka HAI*****

This paper deals with vibrations of a preloaded compliance system as an example of vibrations of nonlinear systems with discontinuities. The resonance curves of harmonic, higher harmonic and subharmonic vibrations are obtained by using the direct numerical integral method presented previously, which is a highly accurate shooting method. Chaos is generated in the system treated here. Influences of amplitude and frequency of external force and damping ratio on the resonance curves and the stability of solutions are discussed. It is found that if a trajectory enters a discontinuous point, a bifurcation is realized. A stable periodic solution becomes unstable due to this bifurcation and chaos may suddenly occur at the halfway point of the period-doubling route. This route to chaos is same as the one found in the forced self-excited vibration system with dry friction.

Key Words: Nonlinear Vibration, Forced Vibration, Chaos, Preloaded Compliance System, Bifurcation, Discontinuity, Harmonic Vibration, Higher Harmonic Vibration, Subharmonic Vibration

1. Introduction

There exist strongly nonlinear vibrating systems with discontinuous characteristics, examples of which are a system with preloaded compliance[1]-[3] which is used in a flexible joint, an earthquake isolation floor[4], an isolator[5], a dot printer[6], and a system accompanied by friction[7]-[9]. Since discontinuity is strongly nonlinear, it is possible that many kinds of nonlinear vibrations occur in such systems. However, because of discontinuities, the analysis of these systems is very difficult and nonlinear vibrations that occur in these systems have not been examined thoroughly. Therefore, we developed the direct numerical integral method[10] which is a shooting method that is able to obtain highly accurate periodic solutions of systems with discontinuities. A forced self-excited system accompanied by dry friction[11] was analyzed by this method. Consequently, discontinuity in the stability of periodic solutions and the route to chaos, which are peculiar to the system with discontinuity, were found and the mechanisms were clarified. A preloaded compliance system also has discontinuity in its restoring force. This system has been investigated for a long time[2], however; subharmonic and higher harmonic vibrations have not been treated. Chaos arising from the discontinuity was found in this system but its mechanism was not clarified[1],[3]. Moreover, it was assumed that the precision of periodic solutions was insufficient and there was an error in the solution[1],[3]. Therefore, we treated a preloaded compliance system and investigated subharmonic vibrations and higher harmonic vibrations in detail using the direct numerical integral method[10]. The effects of the discontinuity of restoring force on the bifurcations of periodic solutions and chaos were examined. It was clarified that the discontinuous restoring force

* Received 8th April, 1998. Japanese original: Trans. Jpn. Soc. Mech. Eng., Vol. 63, No. 615, C(1997), p. 3848-3855 (Received 25th September, 1996)
** Faculty of Engineering, Nagasaki University, 1-14 Bunkyomachi, Nagasaki 852-8521, Japan
*** Faculty of Engineering, Kyushu University, 6-10-1 Hakozaki, Higashi-ku, Fukuoka 812-0053, Japan
**** Fuji Manufacturing, 2-2-3 Shinsaibashi, Chyuo-ku, Osaka 542-0085, Japan
***** Daiwa House, 1-5-16 Awaza, Nishi-ku, Osaka 550-0011, Japan

NII-Electronic Library Service

The Japan Society of Mechanical Engineers

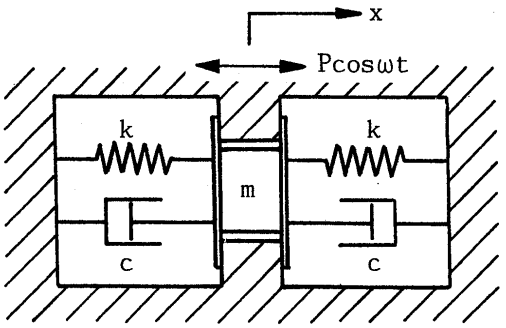

(a) Model

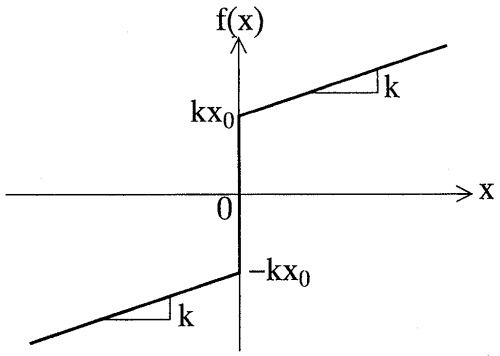

(b) Characteristic of restoring force

Fig. 1 Preloaded system

generated the delta function in the variational equation and that this was the reason for these bifurcations.

2. Theoretical Analysis

2.1 Equation of motion

We consider the one-degree-of-freedom preloaded compliance system shown in Fig. 1(a). This system has mass m, stiffness k and viscous damping coefficient c. The restoring force shown in Fig. 1(b) has discontinuous characteristics at $x=0$ and its value is $2kx_0$. This system is excited by a periodic external force $P\cos\omega t$.

The equation of motion is

$$m\ddot{x}+c\dot{x}+f(x)=P\cos\omega t, \tag{1}$$

where kx_0 is preloaded force,

$$f(x)=k(x+x_0) \quad (x\geq 0)$$
$$f(x)=k(x-x_0) \quad (x\leq 0).$$

Equation (1) may be written in dimensionless form as

$$y''+2\gamma y'+g(y)=p\cos\nu\tau, \tag{2}$$

where

$$g(y)=y+1 \quad (y\geq 0)$$
$$g(y)=y-1 \quad (y\leq 0)$$
$$y=x/x_0,\ \gamma=c/(2\sqrt{mk}),\ \tau=\omega_n t,\ '=d/d\tau,$$
$$\omega_n^2=k/m,\ \nu=\omega/\omega_n,\ p=P/(kx_0).$$

2.2 Numerical calculation method

In general, the analysis of a discontinuous system is difficult. If the system is piecewise linear, we can obtain a periodic solution by connecting the analytical solution of each linear term. However, when the degree of freedom of the system is very large or when we try to obtain higher harmonic vibration, this procedure becomes too complex to obtain periodic solutions. Moreover, if the system is essentially nonlinear, this connecting method is impossible to use. On the other hand, when we integrate the equation of motion numerically, if we do not use any means of maintaining its accuracy, its accuracy decreases to a value proportional to the time step size of integration[12]. Nevertheless, there is a study in which chaos was treated without any means of maintaining accuracy[1]. We developed the direct numerical integral method[10] which is based on the shooting method and can obtain highly accurate periodic solutions of the system with not only continuous nonlinearity but also discontinuous nonlinearity. We confirmed the accuracy of this method and have applied it to a system with discontinuity[11]. We also use this method in this study to obtain periodic solutions and to judge their stability. The outline of the method is given below.

We transform Eq. (2) into a system of two first-order differential equations

$$d\boldsymbol{y}/d\tau=\boldsymbol{f}(\boldsymbol{y},\ t), \tag{3}$$

where

$$\boldsymbol{y}={}^t(y,\ y')={}^t(y_1,\ y_2)$$
$$\boldsymbol{f}={}^t(f_1,\ f_2)={}^t(y_2,\ -2\gamma y_2-g(y_1)+p\cos\nu\tau).$$

Defining the variation of $\boldsymbol{y}$ as $\boldsymbol{\eta}$, the variational equations becomes

$$d\boldsymbol{\eta}/d\tau=\boldsymbol{A}\boldsymbol{\eta} \tag{4}$$

where

$$\boldsymbol{\eta}={}^t(\eta_1,\ \eta_2)$$
$$\boldsymbol{A}=\partial\boldsymbol{f}/\partial\boldsymbol{y}:\text{ Jacobian matrix.}$$

We assume an initial value $\boldsymbol{y}^0$ at $\tau=0$. Then, Eq. (3) is integrated numerically from $\tau=0$ to $\tau=T$, and $\boldsymbol{y}^1={}^t(y_1(T),\ y_2(T))$ is obtained, where $T=2\pi/\nu$. Equation (4) is also integrated numerically from $\tau=0$ to $\tau=T$ with the initial conditions $\boldsymbol{\eta}_1^0={}^t(1,\ 0)$ and $\boldsymbol{\eta}_2^0={}^t(0,\ 1)$, then $\boldsymbol{\eta}_1^1={}^t(\eta_1(T),\ \eta_2(T))$ and $\boldsymbol{\eta}_2^1={}^t(\eta_1(T),\ \eta_2(T))$ are obtained, respectively. As a result, the fundamental solution matrix becomes

$$\boldsymbol{B}=(\boldsymbol{\eta}_1^1,\ \boldsymbol{\eta}_2^1)$$

Since $\boldsymbol{B}=\partial\boldsymbol{y}^1/\partial\boldsymbol{y}^0$, we obtain the first approximate equation with respect to the correction value $\tilde{\boldsymbol{y}}^0$ for $\boldsymbol{y}^0$ by the Newton-Raphson method:

$$(\boldsymbol{B}-\boldsymbol{I}_2)\tilde{\boldsymbol{y}}^0=\boldsymbol{y}^0-\boldsymbol{y}^1 \tag{5}$$

where $\boldsymbol{I}_2$ is a 2×2 unit matrix. We solve Eq. (5) and replace $\boldsymbol{y}^0+\tilde{\boldsymbol{y}}^0$ by $\boldsymbol{y}^0$. The above procedure is repeated until the solution converges. We judge the stability of the convergent solutions using the eingenvalues of

NII-Electronic Library Service

The Japan Society of Mechanical Engineers

matrix $\boldsymbol{B}$, which are called characteristic multipliers. If the absolute values of characteristic multipliers are all less than unity, then the corresponding solution is stable.

Since there is discontinuity in the system, we found a discontinuous point with high accuracy. The integration of the delta function in the variational Eq. (4) was treated as unity.

To obtain a chaotic solution, we used the Runge-Kutta-Gill method with variable time step size and found a discontinuous point with high accuracy. We used a method[10], which was the arranged Shimada-Nagashima's method[13] suitable for a discontinuous system, to obtain Lyapunov exponents.

3. Numerical Results and Discussion

A numerical calculation is carried out using the above-mentioned methods. 1/1, n/1 and 1/n mean harmonic, nth order higher harmonic and 1/n-subharmonic vibrations, respectively, in the figures below. Symbols "O" and "E" in the figures below mean that the periodic solution is composed of odd orders of Fourier series and both odd and even orders of the series, respectively.

3.1 Resonance curves of harmonic and subharmonic vibrations

First, for comparison with the results in Ref. (3), the results for damping ratio $\gamma=0.2$ are shown. Resonance curves of harmonic and subharmonic vibrations are shown in Figs. 2 and 3, respectively. The ordinates represent maximum velocity y'_{max} and the abscissae represent angular velocity ν of the external force. Solid and dashed lines show stable and unstable solutions respectively. All solutions shown here are composed of odd orders of Fourier series and pass the discontinuous point $y=0$ twice in one period. When the amplitude of external force p is large, the resonance curve is similar to that of a linear system, but when the external force p is small ($p=1.2$), the resonance curve exists only in region $\nu>1.1$ and shows multiple values of ν. This means that the smaller the external force is, the stronger the nonlinearity is. This is explained as follows. When the amplitude of external force is small, the amplitude of displacement becomes small; therefore, because of preload, the nonlinearity becomes strong comparatively. We could not find such solutions as those that Shaw and Tung[3] found using the above-mentioned analytical solutions connecting method in region $\nu<1.1$. We consider that their solutions are imaginary ones that do not satisfy the condition that the sign of displacement does not change in every linear region. The existing regions of subharmonic vibration become wide toward smaller ν and the amplitudes of stable solutions become large as external force increases. In a preloaded system, the resonance curves of subharmonic vibrations do not become an island in shape and the upper branches of stable solutions and the lower branches of unstable solutions never intersect each other on the right-hand side. It is assumed that as ν increase, the amplitude of subharmonic vibration decreases, the nonlinearity becomes comparatively strong, and the existing region becomes wide. Chaos is not found in region $\nu>1$.

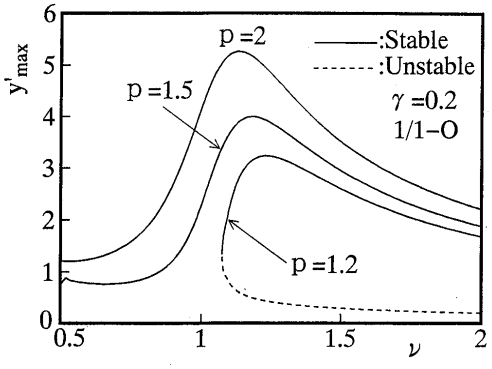

Fig. 2 Harmonic vibration

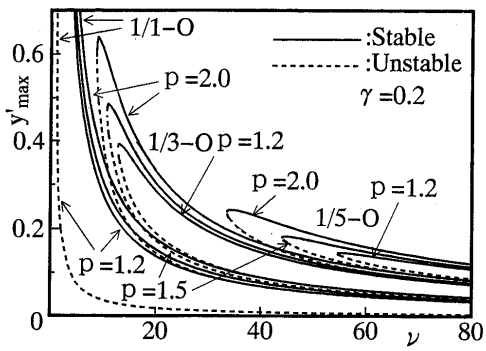

Fig. 3 Harmonic and subharmonic vibration

3.2 Higher harmonic vibrations and chaos

Resonance curves of higher harmonic vibration are shown in Fig. 4. Many types of higher harmonic vibrations occur in region $\nu<1$. As the order of higher harmonic vibration increases, the region in which it exists moves to the lower region of ν. The

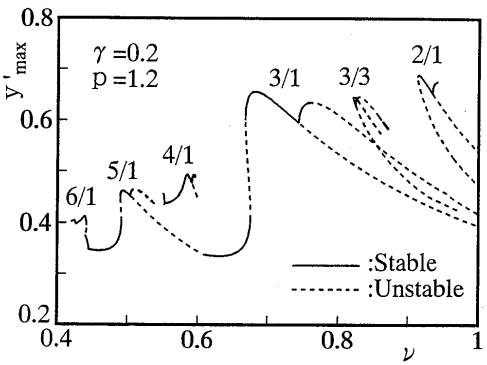

Fig. 4 Higher harmonic vibration

NII-Electronic Library Service

The Japan Society of Mechanical Engineers

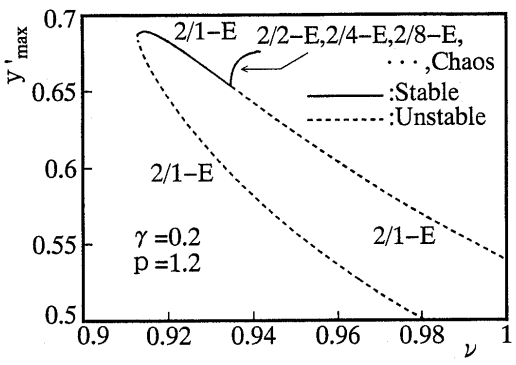

(a) Resonance curve

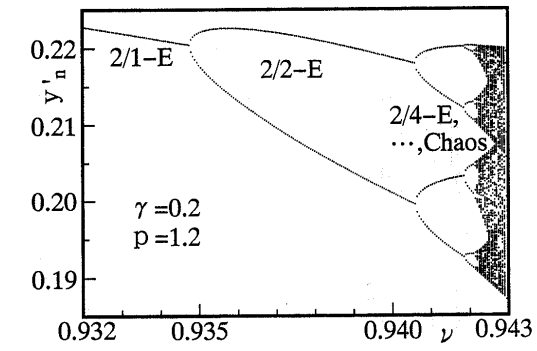

(b) Bifurcation diagram

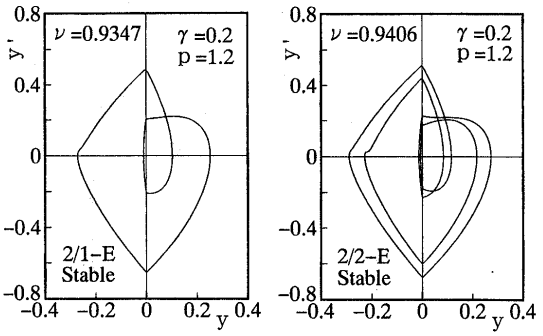

(c) Phase planes

Fig. 5 2nd higher harmonic vibration

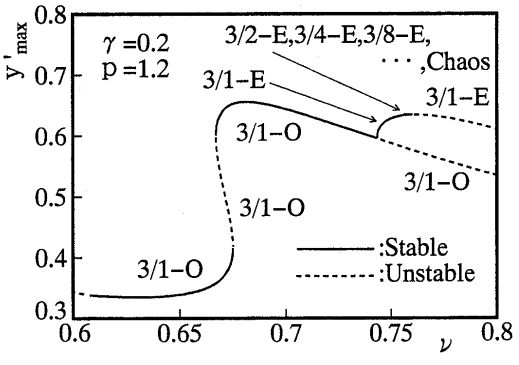

(a) Resonance curve

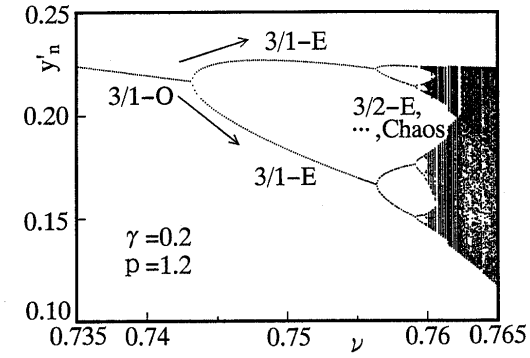

(b) Bifurcation diagram

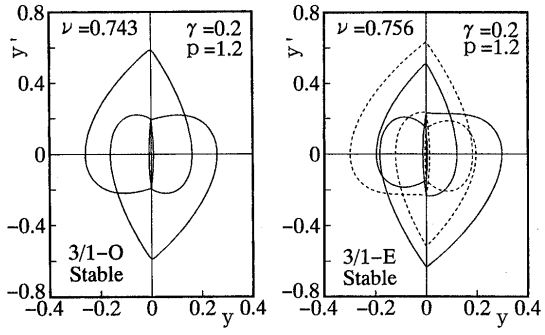

(c) Phase planes

Fig. 6 3rd higher harmonic vibration

value 3/3 in Fig. 4 indicates ultra-subharmonic vibration which is the deformed 3rd higher harmonic vibration and has a period of 6 π/ν.

The magnified the resonance curve, bifurcation diagram and phase planes of the 2nd higher harmonic vibration are shown, respectively, in Figs. 5(a),(b) and(c). The ordinate represents the velocity when the phase of external force is zero and the abscissa represents angular velocity ν of the external force in Fig. 5(b). The ordinate represents the velocity and the abscissa represents displacement in Fig. 5(c). When the order of higher harmonic vibration is even, such as the 2nd higher harmonic vibration, there is no periodic solution composed of only odd orders of Fourier series. The periodic solution 2/1-E composed of both odd and even orders of Fourier series leads to chaos after iterating period-doubling bifurcations. The Lyapunov exponents are 0.004 2 and −0.428 at ν=0.942 1, which means chaos. Since we were able to confirm ultra-subharmonic vibrations up to the 2/64th order by the direct numerical integral method, this route to chaos is assumed to be an ordinary one. The trajectory of periodic solution 2/1-E is not symmetrical with respect to the origin in Fig. 5(c). The figure on the right in Fig. 5(c) is the phase plane of 2/2-E bifurcated in a period-doubling manner from 2/1-E.

The magnified resonance curve, bifurcation diagram and phase planes of the 3rd higher harmonic vibration are shown, respectively, in Figs. 6(a),(b) and(c). The periodic solution 3/1-O bifurcates to 3/1-E and leads to chaos after iterating period-doubling bifurcations. The Lyapunov exponents are 0.001 8

NII-Electronic Library Service

The Japan Society of Mechanical Engineers

and -0.673 at $\nu=0.759\,98$, which means chaos. Since we were able to confirm ultra-subharmonic vibrations up to the 3/64th order by the direct numerical integral method, this route to chaos is assumed also to be an ordinary one. The routes to chaos shown in Figs. 5 (b) and 6 (b) are the same as that of Duffing's equation with restoring force of softening type[14]. The trajectory of periodic solution 3/1-O is symmetrical with respect to the origin in the left figure in Fig. 6 (c). The figure on the right in Fig. 6 (c) is the phase plane of 3/1-E after pitchfork bifurcation of 3/1-O. Solid and dotted lines correspond to the lower and the upper branch in Fig. 6 (b), respectively, which have a phase difference π and the trajectory of 1/3-E is not symmetrical with respect to the origin.

The magnified resonance curve, bifurcation diagram and phase planes of the 4th higher harmonic vibration are shown, respectively, in Figs. 7 (a), (b) and (c). We can see the periodic solution 4/1-E leading to chaos after ordinary period-doubling bifurcations on the right of Fig. 7 (a). We were able to confirm ultra-subharmonic vibrations up to the 4/64th order by the direct numerical integral method. On the other hand, we can see the ultra-subharmonic vibration 4/2-E bifurcating to chaos directly on the left of Fig. 7 (b). The upper branch and the lower one in Fig. 7 (b) have a phase difference π. There exist two small circles to the right of the origin in the left phase plane ($\nu=0.551\,338$) of Fig. 7 (c), whereas the outer circle intersects the origin $y=0$ in the right phase plane ($\nu=0.551\,336$). This is the reason why chaos is generated abruptly. Figure 7 (d) shows the Poincare map of chaos at $\nu=0.551\,336$, which is assumed to be extremely near the bifurcation point. The abscissa represents the velocity y'_n when the phase of external force is zero and the ordinate represents the velocity y'_{n+2} two periods later. We confirmed that the Poincare map does not intersect the diagonal line, from a magnified figure. Dots scatter in the chaos region of Fig. 7 (b). This indicates that this chaos is of the intermittence type. The Lyapunov exponents at $\nu=0.551\,336$ are $0.022\,6$ and -0.748. The characteristic multipliers are $0.768\,9$ and $0.000\,142\,8$ at $\nu=0.551\,336\,567\,446$, which is assumed to be extremely near the bifurcation point and the absolute values of the characteristic multipliers are much less than unity. In an ordinary intermittent route, the absolute value of the characteristic multiplier is equal to unity at the bifurcation point, but in the route to chaos which results from discontinuity of preloaded compliance, it is not equal to unity.

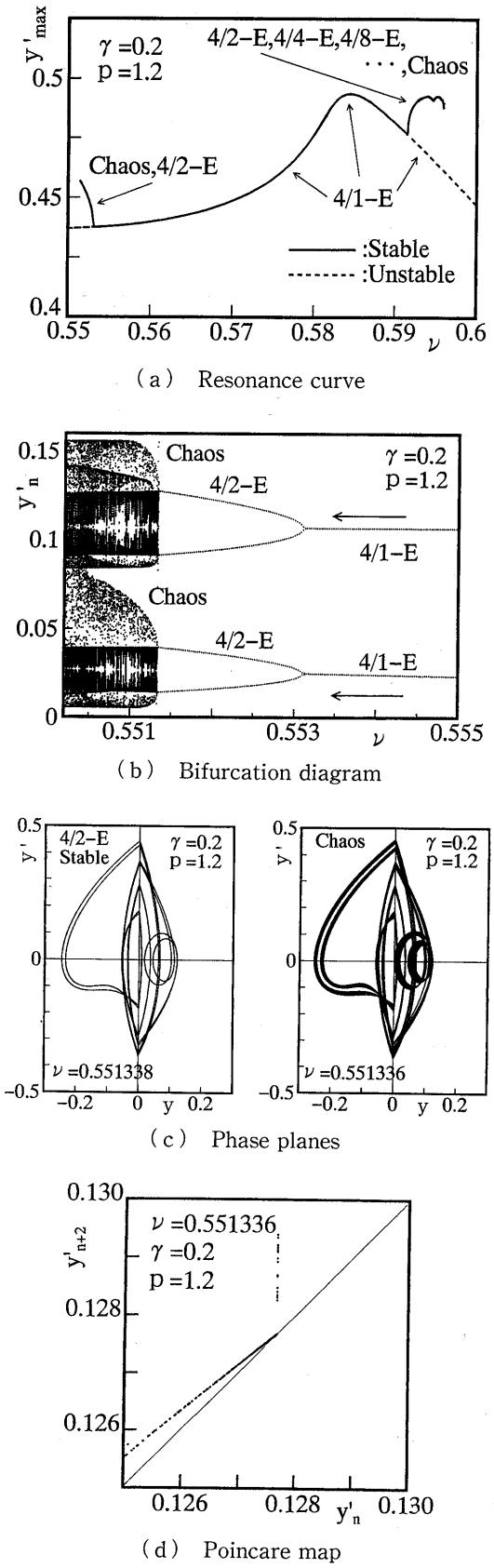

Fig. 7 4th higher harmonic vibration

Numerical results for $\gamma=0.05$, $p=2.0$ are shown in Fig. 8 (a) for comparison with those in Ref. (15). It has been reported that the periodic solution bifurcates discontinuously because of preload (this means discontinuity in resonance curve); however only the stable solutions are calculated in Ref. (15). Therefore, we

NII-Electronic Library Service

The Japan Society of Mechanical Engineers

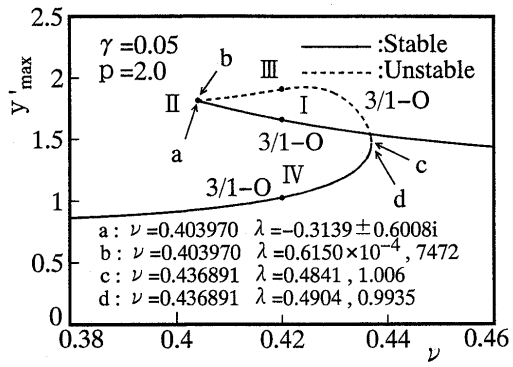

(a) Resonance curve

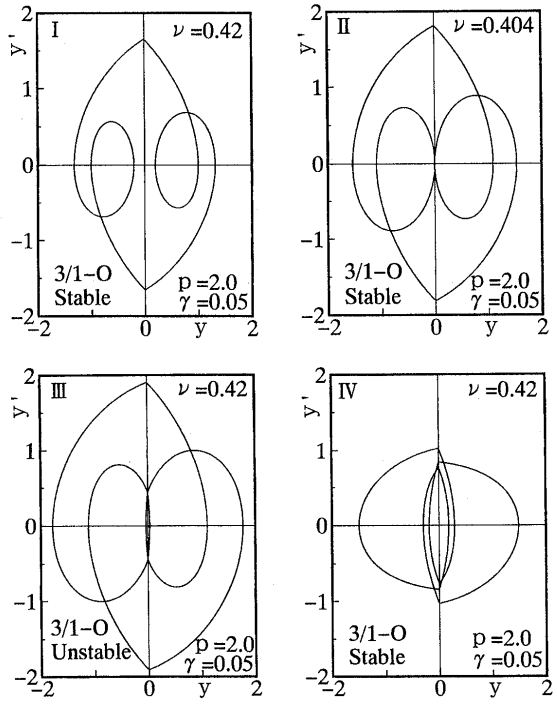

(b) Phase planes

Fig. 8 3rd higher harmonic vibration

attempt to obtain both stable and unstable solutions using the direct numerical integral method in this study. The stable periodic solution 3/1-*O* starting at $\nu=0.46$ changes its inclination from negative to positive discontinuously at the point immediately below $\nu=0.403\,970$; then, it becomes unstable. Two characteristic multipliers change discontinuously before and after this point as follows. They are $-0.313\,9 \pm 0.600\,8i$ at point *a* in the stable solution, 0.000 061 50 and 7 472 at point *b* in the unstable solution, where $i^2=-1$. This unstable solution continues up to the tangent bifurcation point that stands between points *c* and *d*. The inclination at the bifurcation point is vertical and that of characteristic multipliers is unity. Characteristic multipliers before and after the bifurcation point are shown in the resonance curve. The solution becomes the stable 3/1-*O* again after this bifurcation.

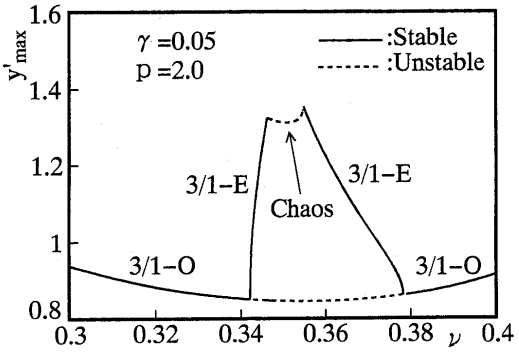

(a) Resonance curve

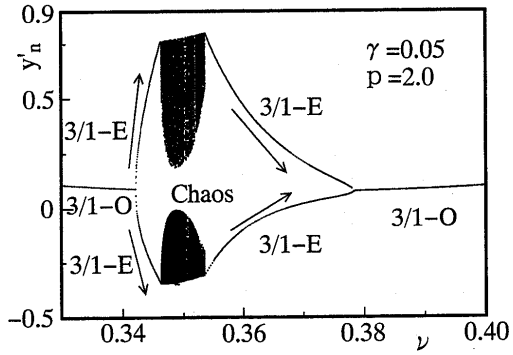

(b) Bifurcation diagram

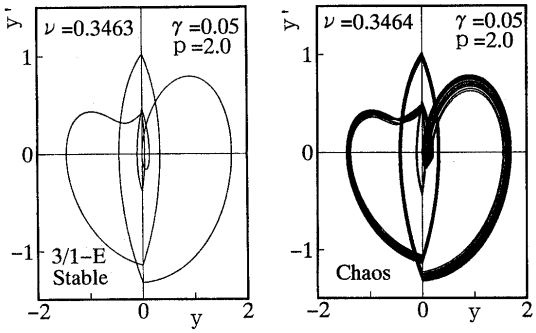

(c) Phase planes

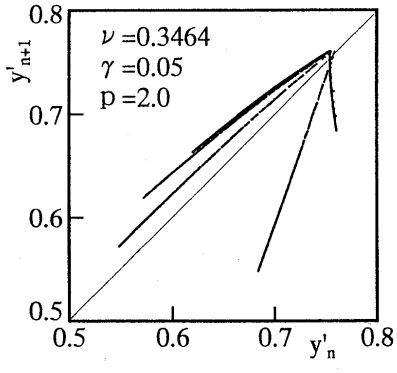

(d) Poincare map

Fig. 9 3rd higher harmonic vibration

Phase planes are shown in Fig. 8(b). Trajectories seen as two circles near the origin in figure I approach the origin which is the discontinuous point of restoring force in figure II, and then intersect with the

NII-Electronic Library Service

The Japan Society of Mechanical Engineers

discontinuous point in figure III. Therefore, the absolute value of the characteristic multiplier jumps over unity at the bifurcation point between points a and b. This indicates the discontinuity in the stability of the periodic solution. The resonance curve is shaped like a bluff at such a bifurcation point.

The resonance curve of 3rd higher harmonic vibration below $\nu=0.4$, the bifurcation diagram, the phase planes and the Poincare map are shown in Figs. 9(a),(b),(c) and (d), respectively. The solution 3/1-O starting from the left end becomes unstable and the stable periodic solution 3/1-E occurs after pitchfork bifurcation at approximately $\nu=0.342$. Then the stable periodic solution 3/1-E becomes unstable and chaos is generated abruptly at approximately $\nu=0.346\,3$. This chaos continues until 3/1-E is generated again at approximately $\nu=0.355\,0$. The characteristic multipliers of the periodic solution are 0.283 7 and 0.093 58 at $\nu=0.346\,3$. The Lyapunov exponents at $\nu=0.346\,4$ are 0.027 6 and -0.316, and the state of vibration is judged as chaos. The phase planes in Fig. 9(c) are those immediately before and after the bifurcation point. We can see a trajectory that is shaped like a small arc on the rightside of the origin in the left figure of Fig. 9(c). On the other hand, in the right figure, the trajectory derived from the above-mentioned one intersects the origin, which is the discontinuous point of restoring force. Therefore, the absolute value of the characteristic multiplier jumps over unity at the bifurcation point. Figure 9(d) shows the Poincare map of chaos at $\nu=0.346\,4$, which is assumed to be beside the bifurcation point. This map is shaped like a bluff, similar to that obtained in the last report[11]. This bluff shape is characteristic of chaos that arises from discontinuity[16].

The phenomena that system behaviors change abruptly depending on whether it passes the discontinuous points are shown above. The mechanism of the phenomena is explained as follows. The variational equation that determines the stability of the solution has a delta function in a system that has a discontinuous function in the equation of motion. The integrated value of the variational equation differs by some amount depending on whether the discontinuous point is passed or not. Therefore, the stability of the solution changes discontinuously and the behavior of the system changes abruptly. As a result, the bifurcations to chaos in Figs. 7(b) and 9 and the change of stability of the periodic solution in Fig. 8 happened

4. Conclusions

We analyzed the harmonic, higher harmonic and subharmonic vibrations of a preloaded compliance system in detail using the direct numerical integral method. Chaos were confirmed in the regions near where the higher harmonic vibrations are generated. It was found that the characteristic multipliers change discontinuously and chaos are generated abruptly because of discontinuity of the restoring force. These characteristics are peculiar to the system with discontinuity.

References

(1) Mahfouz, I.A. and Badrakham, F., Chaotic Behaviour of Some Piecewise-Linear Systems, Part I: Systems with Set-Up Spring or with Unsymmetric Elasticity, J. Sound Vib., Vol. 143, No. 2 (1990), p. 255.

(2) Den Hartog, J.P. and Mikina, S.J., Forced Vibrations with Non-Linear Spring Constants, Trans. Am. Soc. Mech. Eng., J. Appl. Mech., Vol. 54, No. 15(1932), p. 157.

(3) Shaw, S.W. and Tung, P.C., The Dynamic Response of a System with Preloaded Compliance, Trans. Am. Soc. Mech. Eng., J. Dyn. Syst. Meas. Con., Vol. 110(1988), p. 278.

(4) Fujita, T., Hattori, S. and Ishida, J., Research on Earthquake Isolation Floor with Preloaded Spring (1st Report: Basic Study on Base Isolation Device), Trans. Jpn. Soc. Mech. Eng., (in Japanese), Vol. 49, No. 441, C(1983), p. 727.

(5) Natsiavas, S., On the Dynamics of Oscillators with Bi-Linear Damping and Stiffness, Int. J. Non-Linear Mech., Vol. 25, No. 5(1990), p. 535.

(6) Tung, P.C. and Shaw, S.W., The Dynamics of an Impact Hammer, Trans. Am. Soc. Mech. Eng., J. Vib. Acoustics, Stress and Relia., Vol. 110(1988), p. 193.

(7) Den Hartog, J.P., Forced Vibrations with Combined Viscous and Coulomb Damping, Phil. Mag., Vol. 9(1930), p. 801.

(8) Yeh, G.C.K., Forced Vibrations of a Two-Degree-of-Freedom System with Combined Coulomb and Viscous Damping, J. Acoust. Soc. Am., Vol. 39 (1966), p. 14.

(9) Sinha, A. and Griffin, J.H., Effects of Static Friction on the Forced Response of Frictionally Damped Turbine Blades, Trans. Am. Soc. Mech. Eng., J. Eng. Gas Turbines and Power, Vol. 106 (1984), p. 65.

(10) Yoshitake, Y., Sueoka, A., Tamura, H. and Hai, T., Direct Numerical Integral Method to Determine Periodic Solutions of Nonlinear Systems, Trans. Jpn. Soc. Mech. Eng., (in Japanese), Vol. 59, No. 561, C(1993), p. 1428.

(11) Yoshitake, Y., Sueoka, A., Tamura, H. and Shoji, N., Vibrations of Nonlinear Systems with Discontinuities (Case of Forced Self-Excited Vibration Accompanied by Dry Friction), Trans. Jpn. Soc. Mech. Eng., (in Japanese), Vol. 61, No. 583, C (1995), p. 768.

(12) Brown, J.M.B. and Borthwick, W.K.D., A Test Problem for Structural Systems with Discontinu-

NII-Electronic Library Service

The Japan Society of Mechanical Engineers

ities, J. Earthquake Eng. and Struc. Dynam., Vol. 16(1988), p. 135.
(13) Shimada, I. and Nagashima, T., A Numerical Approach to Ergodic Problem of Dissipative Dynamical Systems, Prog. Theor. Phys., Vol. 61, No. 6(1979), p. 1605.
(14) Tamura, H., Kondoh, T., Sueoka, A. and Ueda, N., Higher Order Approximate Solution of Duffing's Equation (Harmonic Resonance of Soft Spring), Trans. Jpn. Soc. Mech. Eng., (in Japanese), Vol. 52, No. 473, C(1986), p. 40.
(15) Imamura, H., Discontinuities Bifurcations and Chaos, Proceedings of Jpn. Soc. Mech. Eng., (in Japanese), No. 890-61(1989), p. 7.
(16) Nusse, H.E. and Yorke, J.A., Border-Collision Bifurcations Including "Period Two to Period Three" for Piecewise Smooth Systems, Physica D, Vol. 57(1992), p. 39.

NII-Electronic Library Service